TECHNOLOGICAL FEATURES IN THE NEW MOLE PENETRATOR "KRET"

Grygorczuk J.[(1)], Seweryn K.[(1)], Wawrzaszek R.[(1)] Banaszkiewicz M.[(1)]

[(1)]Space Research Centre of Polish Academy of Sciences, 18a Bartycka str,00-716 Warsaw, Poland, Email: kseweryn@cbk.waw.pl

ABSTRACT

Mole devices are low velocity, medium to high energy, self-driven penetrators, designed as a carrier of different sensors for *in situ* investigations of subsurface layers of planetary bodies. The maximum insertion depth is limited by energy of single mole's stroke and soil resistance for the dynamic penetration. The principle of operation of a mole bases on the interaction between three masses: the inserted cylindrical casing, the hammer, and the rest of the mass, acting as a support mass. Additionally, the driven spring should act on the hammer and the support, and the return spring should act on the support and the casing.

A new mole penetrator "KRET" has been recently designed, developed, and successfully tested at Space Research Centre PAS in Poland. This approach takes advantage of the MUPUS penetrator (a payload of Philae lander on Rosetta mission) insertion tests knowledge.

Two aspects were critical in development of a new mole: first one is related to the reliability of the mechanisms whereas the second one to the dynamic properties of the penetrator. The specific technological problems i.e. the abrasion and fatigue of the latch, the shape of the tip and proportions between three masses are shown in the paper as an illustration of those aspects. The proper design was confirmed by the operational tests in the testbed system.

1. INTRODUCTION

Surface and subsurface material of planets (and its moons), comets and asteroids often consist of granulated matter with grain size in a range from several μm to several mm, like terrestrial sand. For example, on top of the Moon's crust there is a highly comminuted surface layer of regolith. It has been estimated that the regolith thickness varies from about 3–5 m in the maria, and by about 10–20 m in the highlands [1].

The "mole" penetrometer is an axially symmetric intrusion device, which can move under the surface, discover the properties of the subsurface medium, sample the material, and in some cases, even return to the surface [2] [3] [4]. The mole penetrator can be treated as a transport device for different sensors designed for in situ investigations in subsurface environments [5] [8] [9]. The potential application is connected to scientific investigation (e.g. planetology) [17] but also in lunar exploration and exploitation (e.g. Hel-3 measurements) [18]. Furthermore, the mole penetrator itself can be treated as a precision anchoring device for lunar habitat or other structure on lunar or planetary surface.

Over the recent years, several mole penetrators have been designed and tested in laboratories. Some of them were prepared for a space mission e.g. the one developed by DLR in Cologne for the Beagle 2 lander on ESA Mars Express mission [6], [7]. Another device (the HP3 instrument) is proposed for the ExoMars mission [13].

A new mole penetrator "KRET" has been recently designed, developed, and successfully tested at SRC PAS in Poland [10] [11]. This approach takes advantage of the MUPUS penetrator (a payload of Philae lander on Rosetta mission) insertion tests knowledge [14] [15]. The MUPUS penetrator had four power settings (PS), and the hammer stroke energy at the highest PS4 was over ten times bigger than the one on the PS1 [16]. Insertion tests performed with several porous or granulated materials showed the meaning of the powerful strokes. In development of a new mole, the first (after reliability) priority was to obtain as high as possible ratio: energy of the stroke to the casing cross-section area. This can be provided by a highly energetic spring operating with a reasonable force and long travel. In order to guarantee functionality a new latch mechanism suitable for operation with a long travel helical spring was invented. Among other applied elements in this device, which are commonly used in space mechanisms, the latch was a critical path technology of the mole penetrator. Shaped to a simple form, spring latch was employed to catch the hammer, pull it and release it when the driving spring was fully compressed. The abrasion of different materials on the latch and fatigue effects are presented in this paper.

The dynamics of the mole and, in consequence, the insertion progress depend on proportions between the casing, the hammer and the support mass which in the mole "KRET" case is equal to 1/1/10. For such a challenge materials with very low and very high density for appropriate elements have to be selected. The composite materials (CFRP) and tungsten alloy meet such requirements. The joint between CFRP outer tube and titanium tip of the casing requires to prove the shock resistance on very high peak overloads (10000 g). The results from the test with a usage of two different joints are one of the topics of this paper. Tungsten was used for increasing the mass of the support mass parts.

Proc. '13th European Space Mechanisms and Tribology Symposium – ESMATS 2009', Vienna, Austria 23–25 September 2009 (ESA SP-670, July 2009)

Another improvement comes from numerical simulations [12], which clearly indicate that tips with small angle (15°-30°) penetrates granulated matter better than tips with bigger angles. Unfortunately very small angle caused an increase in total length of the mole penetrator which is not advisable. The best compromise solution was obtained with a nonlinear conical shape (ogive–shaped tip angle starts from 45° at the base and 30° at the end) and such a solution was chosen for our device.

Experiments in the 2m testbed system filed with dry, compacted quartz sand confirm the appropriate design of the mole penetrator "KRET". Up to now we perform several operational tests and we have achieved average penetration speed of about 8.5 mm/stroke.

The paper is organized as follows. First we present the detailed description of the mole penetrator "KRET". In the next two sections we present technological details of the mole and after that the example of the experimental results are given. Finally, the conclusions and future work are presented.

2. PRINCIPLE OF OPERATION

The principle of operation of a mole bases on the interaction between three masses: the inserted cylindrical casing, the hammer, and the rest of the mass, acting as a support mass. Additionally, the driven spring should act on the hammer and the support, and the return spring should act on the support and the casing.

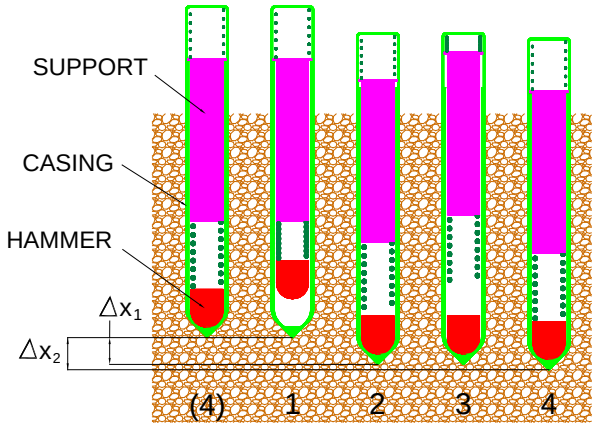

Figure 1 Schematic principle of operation of the mole

In a single work cycle (one stroke) of the mole KRET four phases can be discriminated:

PHASE 1: driven hammer compress the driven spring

PHASE 2: released hammer accelerates and hits the casing. In result of exchange of energy and momentum, the casing is inserted at Δx_1. The support moves in the opposite direction.

PHASE 3: the support reaches the highest position compressing the return spring

PHASE 4: the support accelerated by the return spring and gravity hits the casing and causes its additional move. Then the total progress of insertion for a single work cycle of the mole is Δx_2.

The most of support parts, with exception of the motor, gear and ball screw, were made of tungsten, increasing significantly inertia of the support. Fig 2 presents mechanical parts of which the mole KRET was built.

Figure 2 Mechanical parts of the mole KRET

From the control system's point of view, problems related to mole's operation could be grouped in two areas: (i) detection of critical events in the phases of drive system, (ii) optimal profile of supplying currents and voltages. First problem is directly connected with hammering sequence, which was described in details in previous chapters of the paper. Appropriate control system should behave as follow:

1. connect power supply to motor to realize forward motion of the latch,
2. detect when latch couple the hammer,
3. connect power supply to the motor with opposite polarity to start pulling a driving spring,
4. detect that hammer has been released,
5. short delay before next cycle.

Because of lack of space inside the mole casing, especially in the section where driving mechanism is located, possibilities of introduction any additional sensors are very limited. Finally it was decided not to use any dedicated limit sensors inside the mole and instead of that to use detection and control of the motor current consumption. Forward and backward motion of the latch stops when mechanical limiters are reached. These limiters did not allow mechanism to go further and destroy device. Additionally, high increase of the load torque on the motor's shaft results in high increase of current consumption. This signal could be detected and trigger appropriate control reaction. A LMD18245 full bridge motor driver has been used in our system as a current limiter and motor driver. The circuit bases on Microchip PIC18F2480 microcontroller. Each occurrence when current exceed limit level, an interrupt is generated and microcontroller changes values on appropriate port pins.

3. TECHNOLOGICAL FEATURE 1

During the hammering action cycles, the hammer has to be simultaneously locked and released. This is provided by a special latch mechanism developed for the long travel helical spring. The latch mechanism comprises of two matching parts: the ring lock fixed on the hammer and the latch linearly moved by the ball screw. Proper development of the latch was an especially critical path technology of the mole penetrator. Shaped to a simple form, spring latch was employed to catch the hammer, pull it and release it when the driving spring was fully compressed.

A shape of the latch with forces acting on it and calculated stresses in the material are shown in Fig 3.

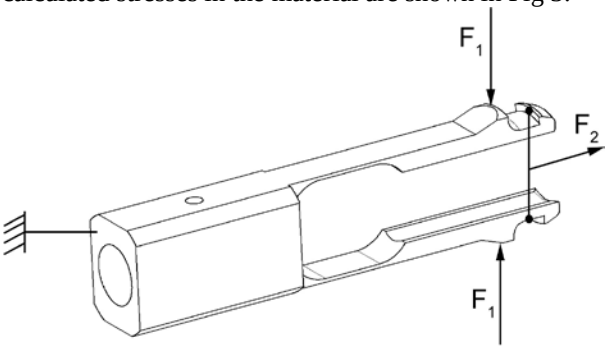

Fig. 3 The constrains and forces acting on the latch: F_1 – bending force needed to squeeze the latch fork, F_2 – pulling force produced by the driving spring

In the TL (technological-laboratory) model of the mole the ring lock (not shown) was made of 440 C stainless steel and hardened. More detailed selection were devoted to the latch material, due to its tinny fork arms which had very good fulfill: strength, elasticity and wear resistance. First approach was focused on the beryllium bronze which possess a unique combination of mechanical strength and elasticity. Critical for hardness and wear resistance areas were coated with hard chromium 25 µm thick. Shortly, it was found out that even the hard chromium was not a good choice for the latch, where intensity of stress was very high on the sharp edges (with R=0.15 mm). After tens of release actions the small cracks visible on the chromed edges have appeared and after additional mechanism actions (very fast) the chrome were completely removed from the working edge (Fig. 4).

In the second approach stainless steel X10CrNi18-8, hardened and tempered was applied. The latch made of this material was successfully used during several insertion tests of the mole with the total number of strokes around 1400, which corresponds to several meters of depth. Inspection of the latch after tests showed that its critical edges looked good and were almost free from abrasions. For the engineering model suitable for work at relevant space environment it is foreseen to use (after prior positive pin on disc test) the nanocrystaline Si_3N_4 (outer zone) + nitrogen austenite, coating layers both on the stainless steel latch and the ring lock.

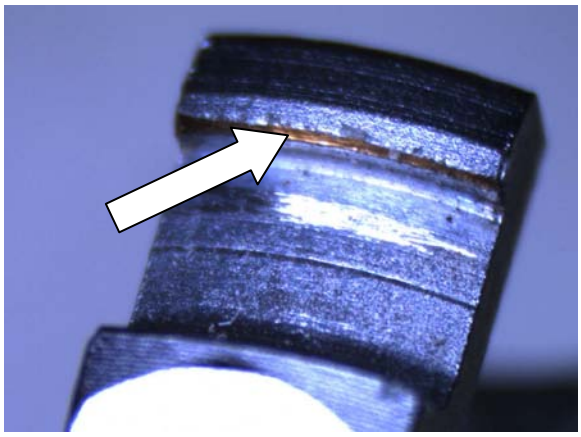

Fig. 4 Final abrasion effects on the latch working edge

The maximum theoretical stress in the latch (Fig. 5) occur when the forces reach the maximum value – in our case F1=5N and F2=120N. The simulation shows that the maximum Von Mises stresses are equal to 442MPa which is below the limit R_m=1400-1600 MPa. The fatigue effect can be checked using the Wöhler curve which gives information on the maximal cyclical stress (S) against the cycles to failure (N). For steel X10CrNi18-8 S=600MPa for N<3000 and S=450 MPa for N<20000 [14]. It means that theoretically the latch cannot operate longer than 20000 cycles [14]. Until now it was experimentally confirmed that latch survived 1400 cycles.

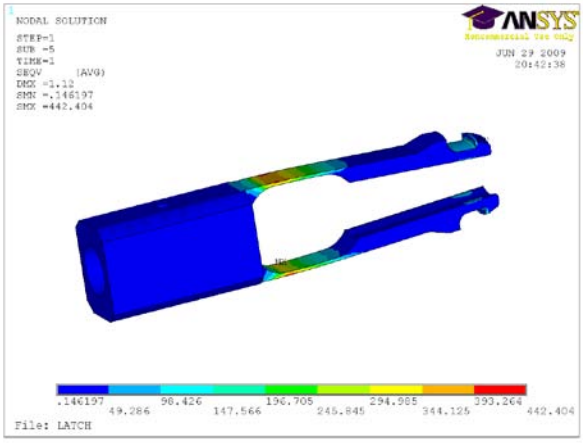

Fig. 5 Von Mises stresses in the latch

The dynamics of the mole and in consequence the insertion progress values, especially at lower gravity conditions, depends on proportions between the casing, the hammer and the support mass, which in the mole "KRET" case is equal to 1/1/10. It is easy to provide a proper mass of the hammer, equal or greater than the mass of the casing. This is principally design dilemma. Optimal masses of the support and casing mostly

depend on materials. Thus, a tungsten alloy and composite material (CFRP), two materials with exceptionally different specific gravity, had to be applied, to obtain the mass of the support ten times higher than the mass of the casing. Lightweight casing was made of the CFRP hollow rod (20.2 mm diameter and 0.8 mm wall thickness) jointed with the hardened titanium tip. That joint had to prove the shock resistance with very high peak overloads (10,000 g). Developed solution of the joint is shown in Fig 6.

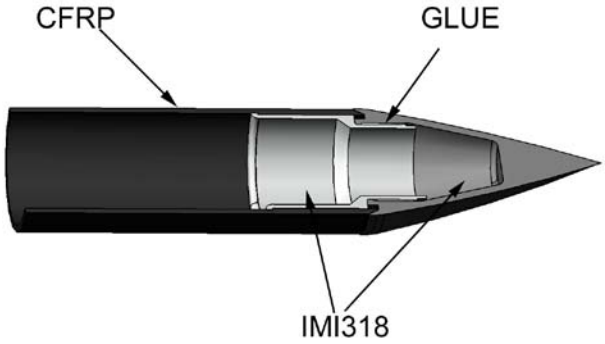

Figure 6 Joints of the CFRP tube with a metal tip

There are two Characteristic features of the joint

1. a 0,3 mm thick and 14 mm long shoulder on the inner CFRP tube surface
2. titanium jointer sleeve with flange from one side and fine thread from the other side

Titanium jointer is inserted into the tube from the rear and glued with Araldite. Titanium tip is screwed with the jointer and also glued with Araldite. Presented lightweight casing, combining CFRP and titanium materials passed all insertion tests of the mole.

4. TECHNOLOGICAL FEATURE 2

The motion sequence of the mole penetrator has been explained in details in section 2 and it is clear that the motion during particular stroke is very short (about 8ms) and its progress highly depends on the effectiveness of energy transfer from the hammer to the surrounded medium. Performed experiments demonstrate that the penetration progress depends on the shape of the mole tip and further detailed numerical analysis confirms this effect.

The penetrator works properly in the granular or porous matter and therefore numerical simulation of the mole motion includes an appropriate physical model of such phenomena. Generally, granular matter behaves like a compressible non-Newtonian complex fluid including fluid solid transition [18] and can be simulated using so called molecular dynamics (MD) simulation [19]. MD simulation dedicated to the penetrator movement analysis was prepared in SRC PAS and is described in details in Ref. 12.

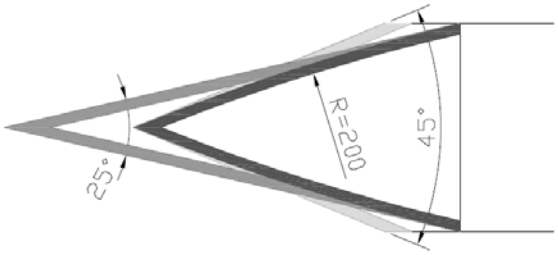

Figure 7 Geometry of three different penetrators tips; the one with 45◦ conical angle (bright line), the one with 25◦ conical angle (mid gray line) and the one which curved conical envelope (circular section with 200 mm radius) (dark line).

All simulations were performed for the following conical angles of the mole tip: 120°, 90°, 60°, 45°, 30° (Fig. 7). Moreover the simulation with a nonlinear conical shape (ogive–shaped tip) was performed. An obvious advantage of a molecular dynamic simulation is that it opens up the possibility of obtaining position, velocity, forces and other dynamical properties of the system at each point and at any time. The most interesting information, however, is the position of the penetrator tip at selected points of time. Therefore, first it is presented the whole system in particular time point (Fig. 8) and then the time evolution of the mole is given in Figure 9.

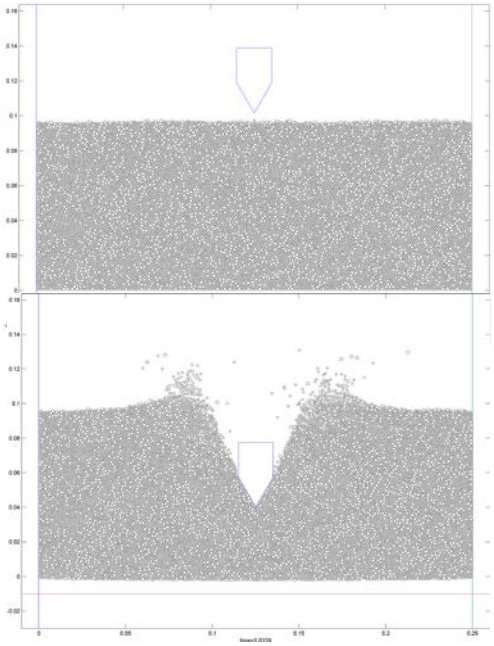

Figure 8 Snapshots of the penetrator motion for two different stages: before impact and during penetration.

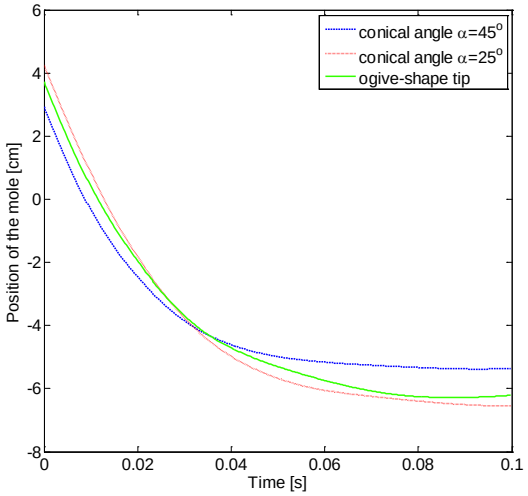

Figure 9 The penetration progress obtained for the tips presented in Fig. 7. The dashed blue line corresponds to the 45° conical angle penetrator, the dotted red line to the 25° conical angle penetrator and solid line corresponds to the ogive–shaped tip.

5. EXPERIMENTAL RESULTS

Insertion tests of the mole has been performed using a special testbed system. The main part of the testbed consists of vertically oriented tube (0.8m in diameter and 2 m length). The tube has been filled up with dry quartz sand (grain size – 0.3-0.8 mm) and in this matter main tests has been performed. Inside the tube, along its length, 10 microphones has been distributed (Fig. 10). This sound detection system was used to get information about position of the mole when it is inside the tube under the surface of sand. To get more accurate information about mole position, four additional microphones were spread in different places inside the tube, but results which were obtained using this kind of sensor network were unsatisfactory. A system with linearly distributed sensors proves to be much more effective. This kind of sensing network was finally used during the tests. Each stroke of mole's hammer was detected by all of sensors. Energy of arriving signal depends on distance between source and detector. Also time of signal traveling could be taken into account, but our experience shows, that this kind of measure is much less accurate and needs more sophisticated equipment. Signal detected by each sensor is gained by dedicated amplifier and registered using National Instruments multi-IO card equipped with LabView software. Because of advanced and computing demanding signal processing, analysis of registered signals has been performed using Matlab software.

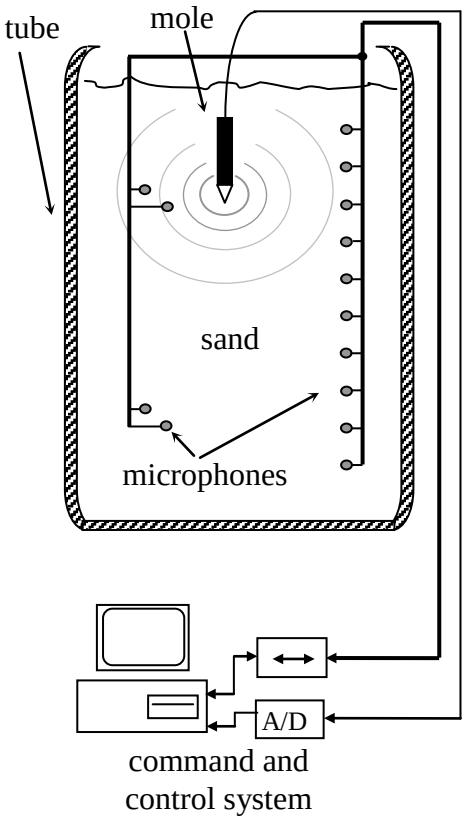

Figure 10 Mole testbed system: tube with dry quartz sand, distributed microphones and command and control system.

Another way to get information about mole position was to measure the length of a cable pulled down under the surface by the mole device. This kind of measure we made manually during a test to check the remote sensing system results.

Final phase of tests took less than 2 hours. During this time the mole has penetrated sand in tube from surface to bottom. Progress of mole descending in relation to stroke numbers is presented on Figure 11.

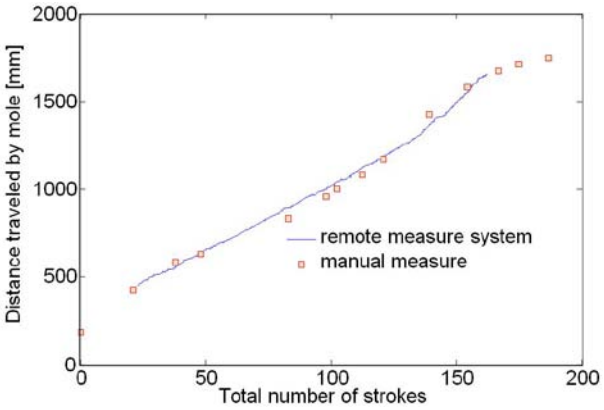

Figure 11 Dependence of insertion progress (distance travelled by mole) versus number of strokes. Characteristics has been obtained during penetration of sand in testbed system (Fig. 10)

It is worth to say, that no considerable decrease of average speed has been detected before the mole started to approach to very close proximity of tube's bottom. Basing on this observation, it is not possible to determine maximum penetration depth directly but we can estimate this value on five - eight meters on Earth.

6. CONCLUSIONS

In the presented paper the technological features of the mole KRET have been briefly described. Assumed goals i.e. reliable latch, the optimal proportions between three interacting masses, stable joints between CFRP and titanium alloy resistant on very high peak overloads and the optimal tip shape have been reached and experimentally proved.
Summarizing the main properties of the mole "KRET" are presented in Tab. 1.

Table 1. The mole KRET measured parameters

Outer diameter [mm]	20.4
Length [mm]	330
Total mass [g]	488
Mass of the inserted casing [g]	46
Mass of the hammer [g]	42
Mass of the support [g]	400
Energy of the driving spring [J]	2.2
Average power consumption [W]	0.28
Average insertion progress per stroke [mm]	8.5
Maximum Penetration Depth [m]	1.85m (testbed limitation)

Future work will be focused on two different approaches towards the mole penetrator problem. First one is focused on the measurements in the new testbed system which allow to insert the mole up to 5m in different space materials analogues. In parallel the test with different inclination will be done. The second aspect concerns developing of the special version of the mole dedicated to lunar environment. This activity is related to the future space mission programs.

7. ACKNOWLEDGEMENTS

The paper was supported from the ESA PECS project no. 98103.

8. REFERENCES

[1] Heiken, G. et al. (1991) (eds.), Lunar Sourcebook, a user's guide to the Moon, 736, Cambridge University Press, New York.
[2] Gromov, V.V. et al. (1997), The Mobile Penetrometer - A "Mole" for sub-surface soil investigation *7th European Space Mechanisms & Tribology Symposium*, ESTEC, Noordwijk.
[3] Kochan H., et al. (2001) The mobile penetrometer (Mole): A tool for planetary sub-surface investigations, *Penetrometry in the Solar System*, Wien.
[4] Lorenz, R.D. and Ball A. J. (2001), Review of impact penetration tests and theories *Penetrometry in the Solar System*, Wien.
[5] Banaszkiewicz, M et al. (2007), A sensor to perform in-situ thermal conductivity determination of cometary and asteroid material *Adv. Space Res. 40(2)* 226-237.
[6] Coste P., (1998) Mobile penetrometer ground tests. *Proceedings of ESA Workshop on Advanced Space Technologies for Robotics and Automation - ASTRA*, ESA/ESTEC, Noordwijk.
[7] Richter L., et al., (2002), Development and testing of subsurface sampling devices for the Beagle–2 lander. *Planetary and Space Science* 50, 903–913,
[8] Dabrowski B and Banaszkiewicz M., (2006) Measurement of Lunar and Martian Regolith Thermal Properties using Subsurface Robotic Teams. *Proceedings of ESA Workshop on Advanced Space Technologies for Robotics and Automation - ASTRA*, ESA/ESTEC, Noordwijk.
[9] Seweryn, K. et al. (2008), Modelling of Passive and Active L-GIP Thermal Measurements in the Lunar Regolith *LPSC XXXIX*.
[10] Wawrzaszek, R. et al. (2009), The Heat-Flow Probe Hardware Component (HPHC) of the LGIP Package *LPSC XL*.
[11] Grygorczuk, J. et al. (2008), Insertion of a Mole Penetrator – Experimental Results *LPSC XXXIX*
[12] Seweryn K., et al. (2009) The micro scale modeling of the interaction of a penetrator with granular medium, *Penetrometry in the Solar System II*, Wien (in press)
[13] Knollenberg J., et al. (2207), Thermal measurements with HP3/TEM on Exo-Mars, *EGU*.
[14] Jui-Hung W. and Chih-Quang L. (2002) Tensile and fatigue properties of 17-4 PH stainless at high temperatures, *Metalurgical and materials transactions A*, Vol. 33(6) 1715-1724.
[15] Spohn, T. et al. (2007), MUPUS – a Thermal and Mechanical Properties Probe for the ROSETTA Lander PHILAE, *Space Sci. Rev*, 128.
[16] Grygorczuk J., et al. (2007): MUPUS insertion device for Rosetta mission. *Journal of Telecommunications and Information Technology* vol. 1/2007
[17] Weinberg, J.D. et al. (2008), Lunar Geophysical Instrument Package (LGIP) I – Science and Instrumentation, *LPSC XXXIX*.
[18] Volfson, D., et al. (2003) Partially fluidized shear granular flows: Continuum theory and MD simulations. *Physical Review E*, 68, 021301.
[19] Luding, S (2004) Molecular Dynamics Simulations of Granular Materials. The Physics of Granular Media, WILEY-VCH Verlag GmbH & Co.KgaA, Weinheim.